Research Article

Guixia Wang*, Junhong Su, and Qingsong Wang

# Study on the duration of laser-induced air plasma flash near thin film surface

https://doi.org/10.1515/phys-2025-0141
received November 18, 2024; accepted March 13, 2025

**Abstract:** The precision of testing the damage threshold of thin film lasers has always been a limiting factor in the advancement of high-power laser systems. The conventional plasma flash method sometimes fails to differentiate between film and air plasma flashes, resulting in significant errors in determining the film damage threshold. By distinguishing between the different durations of thin film and air plasma flashes, misjudgment can be eliminated. The aim of this article is to determine both the calculated and experimental values of the duration of air plasma flash near the surface of thin films ($t_c$) and to analyze the factors that influence it. First, a model is established to calculate the theoretical value of $t_c$. For a sample consisting of a single-layer hafnium oxide film, we assume that the incident laser wavelength, focal spot diameter, energy, and pulse width are 1,064 nm, 0.08 cm, 57.21 mJ, and 10 ns, respectively. The focal length of the lens positioned in front of the film sample is set at 350 mm, with a distance of 5 mm between the film sample and this lens. Under these conditions, the theoretical value for $t_c$ is calculated to be $4.24 \times 10^{-6}$ s. Second, the device was used to conduct eight experiments to obtain experimental values of $t_c$. The results are as follows: (1) An increase in incident laser energy leads to an increase in $t_c$. (2) The length of $t_c$ is solely dependent on the incident laser energy, regardless of the sample material or placement (even when the sample is not placed and the laser directly acts on air). (3) When substituting experiment parameters into the model for calculating $t_c$, there is good agreement between theoretical and experimental values. Third, it was observed that $t_c$ increases with increasing incident laser energy, pulse width, and focal length of the lens, while decreasing with an increase in distance between the film sample and the lens.

**Keywords:** laser damage, air plasma flash, duration of air plasma flash, damage threshold

## 1 Introduction

The thin film element plays a crucial role in high-energy laser systems and must have excellent resistance to laser damage. The quality of its resistance to laser damage is usually assessed by the laser-induced damage threshold (LIDT), where a higher LIDT indicates superior resistance to laser damage, while a lower LIDT signifies diminished protective capability against laser-induced harm [1–4]. As laser technology advances toward higher energy levels [5,6], achieving high LIDT is very important to improve the damage resistance of optical element. Precise measurement of LIDT for these elements is key to addressing this challenge. When evaluating the LIDT of optical element following ISO 21254, it is essential to accurately determine if each test point has experienced damage [7]. The traditional method for identifying damage through plasma flashes may struggle to distinguish between air and thin film plasma flashes, potentially leading to misinterpretations and significant errors in assessing the thin film's damage threshold. Additionally, integrating a thin film component into a high-energy laser system may result in premature damage, ultimately compromising the system's overall functionality.

When using the traditional plasma flash method for identifying damage, there are cases where it is unable to distinguish between air and thin film plasma flashes, potentially leading to incorrect assessments. To improve the precision of identifying film damage and avoid such misunderstandings, it is crucial to differentiate between air and film plasma flashes. A study in 2011 [8] found that during experiments involving a laser interacting with a target, the duration of the target's plasma flash was around 280 ns, while the duration of the air's plasma flash was over 7,580 ns. Therefore, by measuring both the

* **Corresponding author: Guixia Wang,** Department of Photoelectric Engineering, Xi'an Technological University, 2 Xue fu zhong lu, Wei yang District, Xi'an, Shaanxi, 710021, China, e-mail: noragirl6@126.com
**Junhong Su**, **Qingsong Wang:** Department of Photoelectric Engineering, Xi'an Technological University, 2 Xue fu zhong lu, Wei yang District, Xi'an, Shaanxi, 710021, China

plasma flash duration of the film ($t_F$) and that of air ($t_c$), one can effectively tell these two types of flashes apart. This distinction will help prevent misjudgments and enhance accuracy in identifying film damage.

Currently, extensive research has been conducted on the formation process and mechanisms of laser-induced plasma flashes in air. It has been reported [9,10] that the growth and formation stages of air plasma have been studied by using the cascade ionization theory, and four different stages of air plasma composition have been proposed, and ignition occurs after the second stage. Several other literature [11–15] have studied the space-time evolution behavior of the plasma flash phenomenon caused by laser-induced air breakdown, and found that the air plasma appears as a luminous droplet in space, expanding in the opposite direction of the laser beam, lasting only tens of microseconds, and then dissipated. Liu *et al.* [16] studied the effect of gas pressure on the properties of air plasma through the experiment of laser-induced plasma emission spectrum, identifying rules governing gas pressure's effects on emission spectrum intensity, electron temperature, and electron density within the air plasma. While most studies aim to elucidate phenomena related to time-space evolution during an air plasma flash, challenges remain regarding accurate calculation and measurement of the air plasma flash's duration ($t_c$).

In this study, the length of $t_c$ is studied theoretically and experimentally, and the factors affecting it are discussed. The specific contents include: (1) Creating a model for calculating $t_c$; (2) Obtaining experimental values for $t_c$, then comparing and analyzing these results with theoretical predictions; and (3) Investigating relevant factors influencing $t_c$ through analysis using the established model to determine their influence patterns.

## 2 Theoretical model

In general, thin film plasma is typically generated using air plasma. Once the plasma is created, it absorbs laser energy and undergoes a rapid temperature increase. This sharp rise in temperature leads to the expansion of the volume outward, resulting in the formation of laser-supported detonation waves (LSDW). The emergence of LSDW causes alterations in surface pressure on the film. At time $t = 0$, when the laser is not working, its surface pressure is at initial atmospheric pressure $p_0$. Upon application of the laser and as a result of LSDW effects, the surface pressure rapidly increases from $p_0$ and then decreases until reaching $p_0$ again. The duration for this entire process is defined as $t_0$ – the action time associated with LSDW.

There are four stages in the formation and development of air plasma. The first stage is the initial phase, where initial electrons are produced after laser irradiation at the focal point, indicating the beginning of flash occurrence. The second stage involves rapid formation of plasma; during this phase, cascade ionization leads to a rapid increase in ions and free electrons within the air, resulting in reaching a critical threshold of the electron density near the focal point. The combined duration of both the first and second stages is known as the flash's ignition time ($t_b$). The third stage includes development accompanied by shock wave propagation from the air plasma near the focusing area. Finally, in the fourth stage, there is a dissipation of plasma. The flash's ignition time is defined as the total duration of both the first and second stages. The sum of the duration of the third and fourth stages is defined as the duration of the air plasma $t_c$. Then,

$$t_c = t_0 - t_b. \tag{1}$$

According to Wang and Su [17],

$$t_0 = t_{2D}\left(\frac{\left(\rho_0 \frac{v_L^2}{\gamma_b+1}\left(\frac{\gamma_b+1}{2\gamma_b}\right)^{\frac{2\gamma_b}{\gamma_b-1}}\right)\left(\frac{t_p}{t_{2D}}\right)^{\frac{2}{3}}}{p_0}\right)^{\frac{5}{6}}. \tag{2}$$

where $t_p$ represents the width of the laser pulse, while $t_{2D}$ denotes the characteristic time for the two-dimensional motion of LSDW. $v_L$ stands for the propagation speed of LSDW, $\rho_0$ represents air density, $\rho_0 = 1.295\ \text{kg/m}^3$, $\gamma_b$ is the adiabatic index of the plasma and $\gamma_b = 1.2$ in the plasma region. The film's surface pressure is initially set at atmospheric pressure $p_0$, and $p_0 = 1.013 \times 10^5\ \text{N/m}^2$.

When the incident laser having a wavelength of 1,064 nm, a focusing diameter of 0.08 cm, energy of 57.21 mJ, a pulse width of 10 ns, is focused by a lens with 350 mm focal length, and is focused 5 mm away from the sample surface, it interacts with a single layer of hafnium oxide film with $t_0 = 4.24 \times 10^{-6}$ s.

According to literature [18], $t_b$ is on the order of tens of nanoseconds, which can be ignored compared with the order of microseconds of $t_0$. Hence,

$$t_c \approx t_0 = t_{2D}\left(\frac{\left(\rho_0 \frac{v_L^2}{\gamma_b+1}\left(\frac{\gamma_b+1}{2\gamma_b}\right)^{\frac{2\gamma_b}{\gamma_b-1}}\right)\left(\frac{t_p}{t_{2D}}\right)^{\frac{2}{3}}}{p_0}\right)^{\frac{5}{6}}. \tag{3}$$

It is obvious that $t_c \approx 4.24 \times 10^{-6}$ s, this is consistent with the conclusion in the study by Chen *et al.* [8]: The air plasma flash lasts for more than 7,580 ns.

# 3 Experimental study

## 3.1 Principle of experimentation

The Nd:YAG laser 1 emits a laser beam, which passes through light filter plate 2 and attenuator 3 in sequence. The laser passes through the focusing system 4 to the beam splitter 5, one beam to the sample platform 7, and the other beam is connected to the energy meter 6 to measure the energy reaching 7 in real time. Computer 8 is the console of the entire system. The laser operates at a wavelength of 1,064 nm with adjustable output energy ranging from 5 to 235 mJ. The diameter of the focused spot measures approximately 0.08 cm, and it has a pulse width of 10 ns. Detectors 9 and 10 are high-speed free-space photodetectors, DET08CL/M and DET025AL/M, respectively, both manufactured by THORLABS, capable of collecting spectral ranges of 800–1,700 nm and 400–1,100 nm, respectively. The incident laser signal and the air plasma flash signal were captured by detectors 9 and 10, respectively. The light signal of detector 9 is the signal that triggers the operation of detector 10. The resulting light signals are then converted into electrical signals, which are displayed using the RT01014 four-channel oscilloscope 12 produced by Rohde & Schwarz Company. Oscilloscope 12 has a bandwidth of up to 1 GHz and a sampling rate of 10 GHz. Consequently, the duration of the voltage signal displayed by detector 10 on the oscilloscope 12 is the duration of the air plasma flash $t_c$. In order to prevent the high energy laser from damaging the detector 9, the attenuator group 11 is placed in front of the detector 9 to protect it (Figure 1).

## 3.2 Results and analysis

Eight experiments were carried out to measure the air flash's duration. For experiments 1–3, a one-layer $Al_2O_3$ film of $\lambda/4$ optical thickness was used as the sample, and the laser energies used were 92.076, 80.567, and 69.057 mJ, respectively. Figures 2–4 display the output signals, from which the durations of the air plasma flashes ($t_c$) are determined to be 5.88, 5.38, and 5.25 μs, respectively. For experiments 4–6, a one-layer $SiO_2$ film of $\lambda/4$ optical thickness was used as the sample, and the laser energies used were 238.41, 95.364, and 52.038 mJ, respectively. Figures 5–7 display the output signals, from which the durations of the air plasma flashes ($t_c$) are determined to be 13.63, 6.99, and 4.08 μs, respectively. In experiment 7, a one-layer $HfO_2$ film of $\lambda/4$ optical thickness was used as the sample, and laser energies used was 57.21 mJ. The output signal shown in Figure 8 depicts the flash's duration ($t_c$) to be around 4.23 μs. In experiment 8, no sample is placed, the laser was directly applied to ambient air using an incident energy level also set at 231.79 mJ. The resulting output signal is

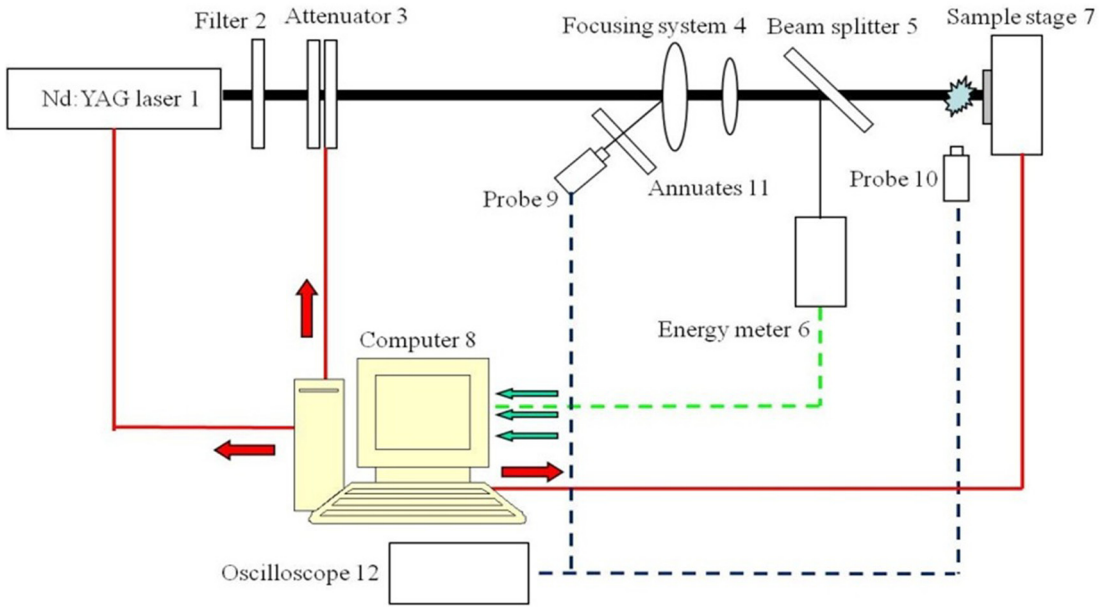


**Figure 1:** Diagram illustrating the experimental setup.

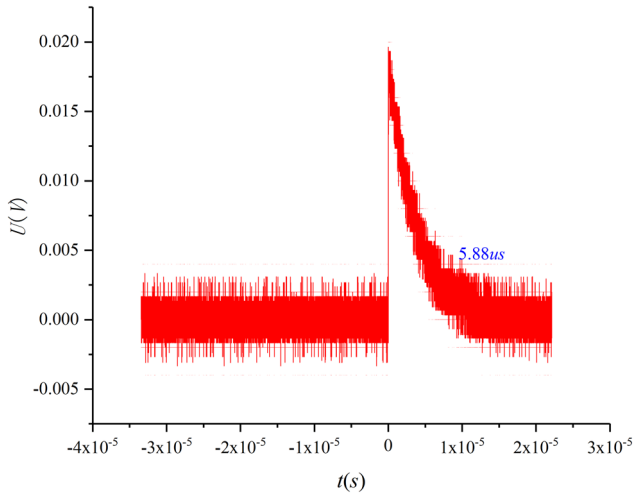


**Figure 2:** Signal diagram of Experiment 1 ($Al_2O_3$ thin film, laser energy is 92.076 mJ).

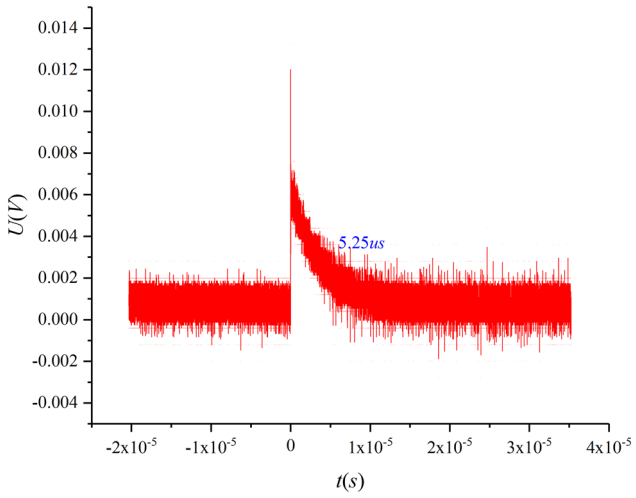


**Figure 4:** Signal diagram of Experiment 3 ($Al_2O_3$ thin film, laser energy is 69.057 mJ).

depicted in Figure 9. Consequently, the length of time the air plasma flash lasts ($t_c$) observed here is estimated to be around 12.06 μs.

The $t_c$ in Figures 2–9 is summarized in Table 1. It can be observed from Table 1 that from experiment 1 to experiment 8, $t_c$ increases with the increase in laser energy. Experiments 1 and 5 have similar laser energy, resulting in comparable $t_c$ values. Similar conclusions are also drawn for experiments 6 and 7, indicating that the $t_c$ is not dependent on the sample material. In experiments 4 and 8, where the incident laser energy is similar but the sample differs ($SiO_2$ film for experiment 4 and no sample for experiment), similar $t_c$ values are obtained, suggesting that whether a sample is present or not does not influence the $t_c$.

This is because according to the analysis in Section 2.1, when the sample is placed on the sample table, the pressure on the film's surface consists of three parts, and the part related to the sample material is only the pressure generated by the ejecting material on the sample surface. The mass of this spatter is so small that the pressure generated is negligible. Therefore, the length of time $t_c$ is independent of whether the sample is placed or not, and also independent of the material in which the sample is placed.

The following are the relevant parameters of the experiment: Assuming that the laser having a wavelength of 1,064 nm, a diameter of focusing spot of 0.08 cm, a pulse width of 10 ns is focused by a lens with 350 mm focal

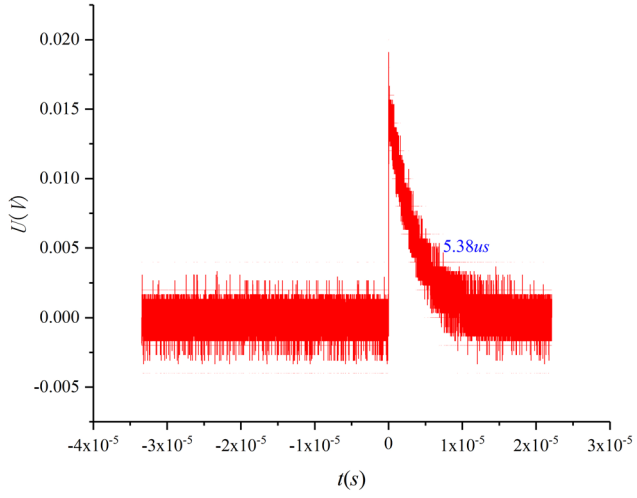


**Figure 3:** Signal diagram of Experiment 2 ($Al_2O_3$ thin film, laser energy is 80.567 mJ).

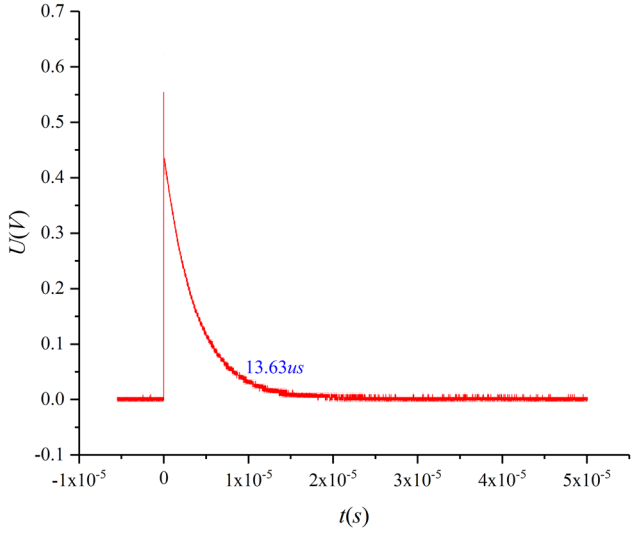


**Figure 5:** Signal diagram of Experiment 4 ($SiO_2$ thin film, laser energy is 238.41 mJ).

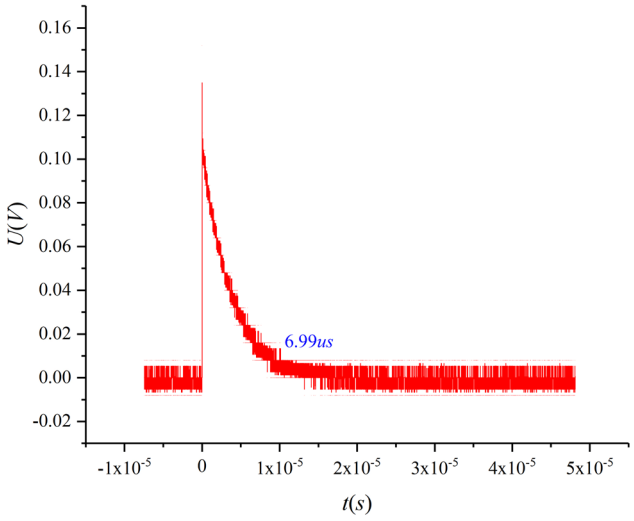


**Figure 6:** Signal diagram of Experiment 5 ($SiO_2$ thin film, laser energy is 95.364 mJ).

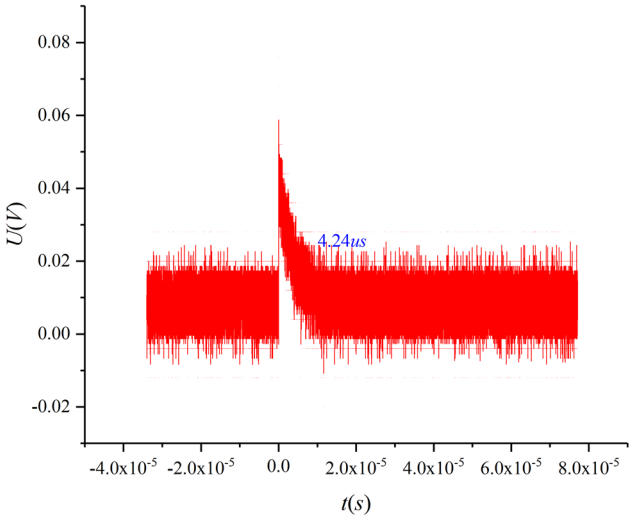


**Figure 8:** Signal diagram of Experiment 7 ($HfO_2$ thin film, laser energy is 57.21 mJ).

length, and is focused 5 mm away from the sample surface, when the laser energy $E$ matches the experimental values listed in Table 1, theoretical values ($t_c$) for various samples at different $E$ levels can be calculated using Eq. (3), and the outcomes are presented in Table 1.

Table 1 shows that, with the exception of experiments 4 and 8, the results of calculation and experiment of $t_c$ are in close agreement. The disparity between the results of calculation and experiment in experiments 4 and 8 may be attributed to air breakdown by high-energy lasers before reaching the film surface [19], resulting in a prolonged plasma flash duration and a larger experimental value of $t_c$ compared to the theoretical value.

In summary, the theoretical and experimental values of $t_c$ both support the conclusion that

(1) $t_c$ increases with increasing laser energy $E$; (2) The length of $t_c$ only depends on incident laser energy regardless of whether a sample is placed or its material type; (3) The theoretical findings align well with the experimental $t_c$ values.

## 4 Analysis of influencing factors

The $t_c$ is affected by a range of factors, such as ambient conditions like pressure, humidity and temperature, the

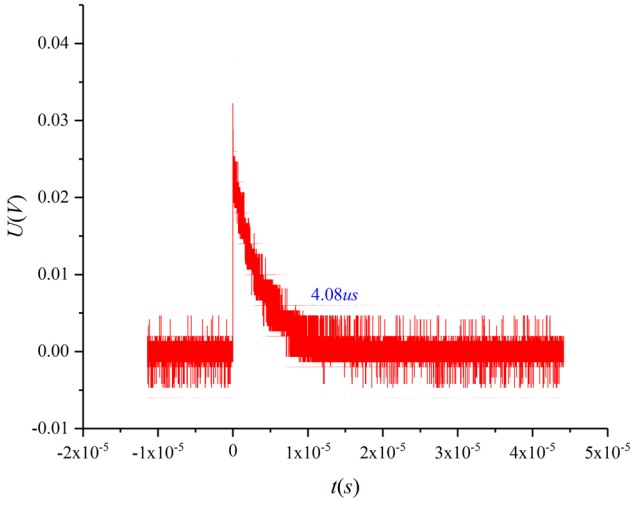


**Figure 7:** Signal diagram of Experiment 6 ($SiO_2$ thin film, laser energy is 58.038 mJ).

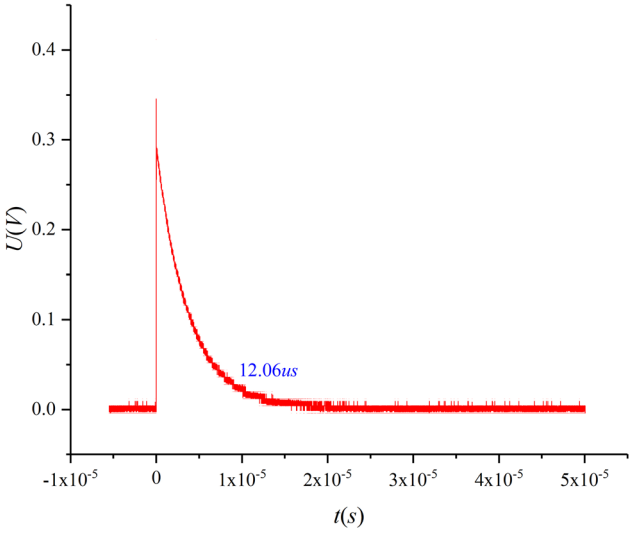


**Figure 9:** Signal diagram of Experiment 8 (air, laser energy is 231.79 mJ).

**Table 1:** Experimental and theoretical values of $t_c$

| Experimental number | Sample | $E$ (mJ) | Experimental $t_c$ (μs) | Theoretical $t_c$ (μs) |
|---|---|---|---|---|
| 1 | $Al_2O_3$ film | 92.076 | 5.88 | 5.93 |
| 2 | $Al_2O_3$ film | 80.567 | 5.38 | 5.62 |
| 3 | $Al_2O_3$ film | 69.057 | 5.25 | 5.27 |
| 4 | $SiO_2$ film | 238.410 | 13.63 | 8.74 |
| 5 | $SiO_2$ film | 95.364 | 6.99 | 6.01 |
| 6 | $SiO_2$ film | 52.038 | 4.08 | 4.47 |
| 7 | $HfO_2$ film | 57.210 | 4.24 | 4.88 |
| 8 | Not any (air) | 231.790 | 12.06 | 8.64 |

laser parameters, and focusing parameters. Assuming that electron adhesion and diffusion can be ignored, and that the design and preparation of focusing parameters and environmental conditions are reasonable, the main influences on $t_c$ are the energy ($E$), the distance between the focal plane and the sample surface ($z_0$), the lens' focal length ($f$), and the width of laser pulse ($t_p$).

The variation in $t_c$ will be investigated when the energy ($E$), the distance between the focal plane and the sample surface ($z_0$), the lens' focal length ($f$), and the width of laser pulse ($t_p$) change.

## 4.1 Laser energy

When the energy $E$ is varied while keeping other parameters constant ($t_p$ = 10 ns, $f$ = 350 mm, $z_0$ = 5 mm), the variation curve of $t_c$ can be obtained, as shown in Figure 10. It is evident from Figure 10 that $t_c$ increases with an increase in $E$, and $t_c$ is on the order of microseconds.

Holding all other factors constant, higher laser energy results in increased absorption of laser energy by air. This results in an earlier generation of air ionization, which results in a faster generation of high-temperature, high-density plasma. The plasma then rapidly absorbs remaining laser energy, expands quickly, and forms the plasma flash at an accelerated rate. In addition, $t_c$ is prolonged due to the enhanced absorption of laser energy by the plasma.

## 4.2 Distance between the focal plane and the sample surface

When the distance between the focal plane and the sample surface ($z_0$) is adjusted while keeping other parameters constant ($t_p$ = 10 ns, $f$ = 350 mm, $E$ = 100 mJ), the variation curve of $t_c$ can be obtained, as shown in Figure 11. It is evident from Figure 11 that $t_c$ decreases with an increase in $z_0$, and $t_c$ is on the order of microseconds.

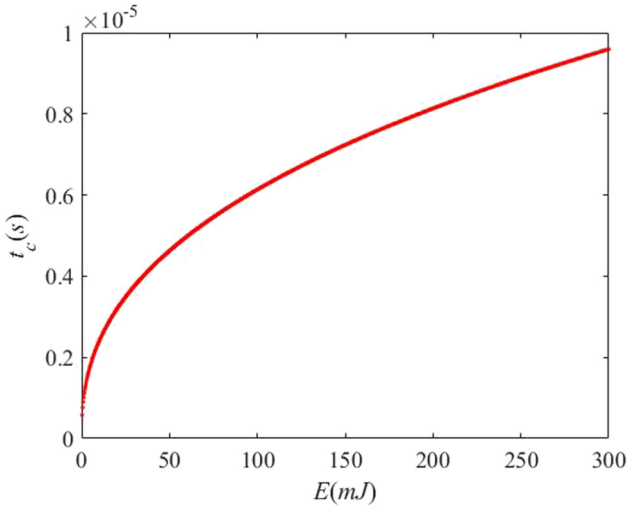


**Figure 10:** Curve of $t_c$ *vs* $E$ ($t_p$ = 10 ns, $f$ = 350 mm, $z_0$ = 5 mm).

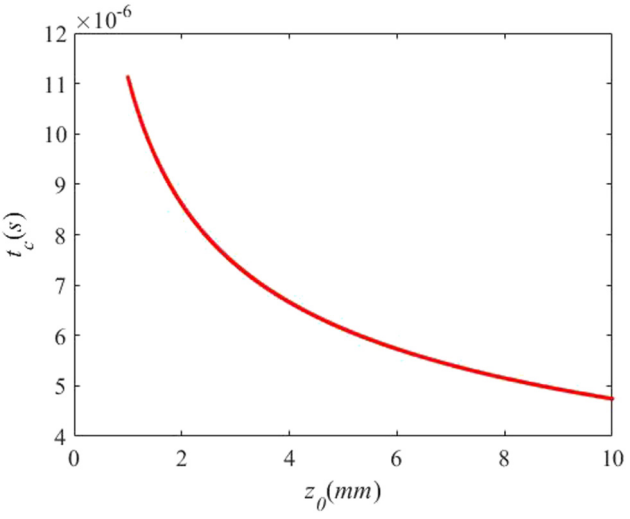


**Figure 11:** Curve of $t_c$ *vs* $z_0$ ($t_p$ = 10 ns, $f$ = 350 mm, $E$ = 100 mJ).

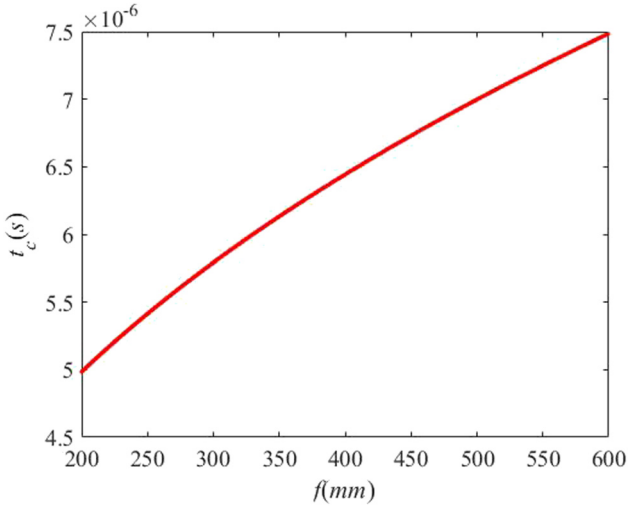


**Figure 12:** Curve of $t_c$ *vs* $f$ ($t_p$ = 10 ns, $z_0$ = 5 mm, $E$ = 100 mJ).

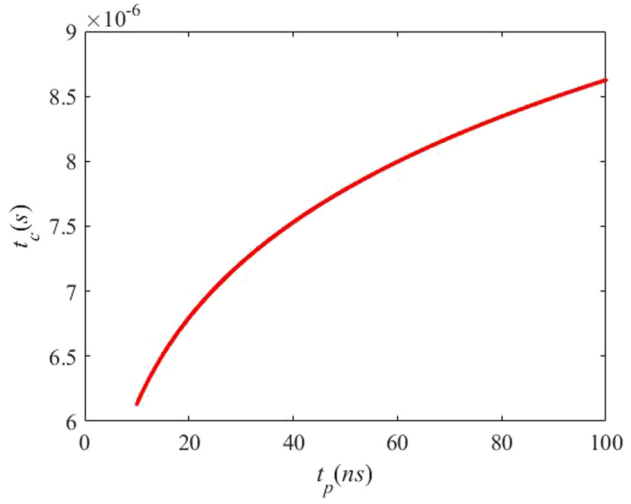


**Figure 13:** Curve of $t_c$ *vs* $t_p$ ($f$ = 350 mm, $z_0$ = 5 mm, $E$ = 100 mJ).

The wider the distance between the focal plane and the sample surface due to Gaussian laser energy distribution, the larger the area of the laser spot acting on the sample, results in a decrease in laser energy per unit area. As a result, the plasma production is slower, and the laser energy absorbed by the plasma is also reduced, ultimately leading to a shorter $t_c$.

### 4.3 Focal length of lens

When the lens' focal length ($f$) is adjusted while keeping other parameters constant ($t_p$ = 10 ns, $z_0$ = 5 mm, $E$ = 100 mJ), the variation curve of $t_c$ can be obtained, as shown in Figure 12. It is evident from Figure 12 that $t_c$ increases with an increase in $f$, and $t_c$ is on the order of microseconds.

The size of the focusing spot is influenced by the change in $f$. A smaller $f$ leads to a larger focusing spot, resulting in a larger laser spot on the surface of the film. This leads to a decrease in laser energy per unit area, resulting in less blockage generated by plasma and less laser energy absorbed, thereby shortening the $t_c$.

### 4.4 Width of laser pulse

When the width of laser pulse $t_p$ is varied while keeping other parameters constant ($f$ = 350 mm, $z_0$ = 5 mm, $E$ = 100 mJ), the variation curve of $t_c$ with $t_p$ can be obtained, as shown in Figure 13. It can be observed from Figure 13 that $t_c$ increases with an increase in $t_p$, and $t_c$ is on the order of microseconds.

When the width of laser pulse is reduced, the laser power increases and the laser power density reaches the threshold for air plasma ignition more quickly under unchanged conditions. As a result, the plasma flash occurs at a faster rate, absorbs more laser energy, and has a longer duration.

## 5 Conclusion

1) A theoretical model has been formulated to calculate the $t_c$. When $\lambda$ = 1,064 nm, $D_s$=0.08 cm, $t_p$ = $10^{-8}$ s, $z_0$ = 5 mm, $f$ = 350 mm, and $E$ = 57.21 mJ, the $t_c$ of hafnium oxide thin films is 4.24 × $10^{-6}$ s.
2) The value of $t_c$ is determined through experimentation, and the parameters in the experimental study are substituted into the established model, and the corresponding $t_c$ theoretical values are calculated. Analysis of both the experimental and theoretical values leads to the following conclusions: (1) As incident laser energy increases, so does $t_c$; (2) The duration of $t_c$ depends solely on incident laser energy, regardless of sample placement or material type. (3) Theoretical results closely match experimental $t_c$ values.
3) After conducting calculations and analysis, it was determined that the increase in $E$, $f$, and $t_p$ leads to an increase in $t_c$, while a decrease in $z_0$ results in a decrease in $t_c$. The process of generating plasma flash through laser-induced breakdown thin film is intricate. This study specifically examines the individual impacts of $E$, $f$, $t_p$, and $z_0$ on $t_c$. Additionally, other factors such as ambient gas pressure, temperature, humidity, pre-ionization, and type also have an influence on $t_c$ in reality. These factors will be the focus of future research.

4) The initial step in distinguishing between the duration of air plasma flash ($t_c$) and film plasma flash ($t_f$) is to acquire both experimental and theoretical values for $t_c$. Once $t_c$ is determined, it becomes feasible to differentiate between the two flashes, thereby reducing misinterpretation caused by the plasma flash method when evaluating laser film damage.

**Funding information:** This work was supported in part by National Natural Science Foundation of China (NSFC) and Shaanxi Provincial Natural Science Basic Research Program Project (No. 62205263, No. 61378050, and No. 2023-JC-QN-0723).

**Author contributions:** G.W.: validation, formal analysis, visualization, experiment, writing – original draft, writing – review and editing, and data curation. J.S.: conceptualization, methodology, software, investigation, writing – review and editing, supervision, and data curation. Q.W.: software and investigation. All authors have accepted responsibility for the entire content of this manuscript and approved its submission.

**Conflict of interest:** The authors state no conflict of interest.

**Data availability statement:** All data that support the findings of this study are included within the article.

# References

[1] Xie LY, Zhang JL, Zhang ZY. Rectangular multilayer dielectric gratings with broadband high diffraction efficiency and enhanced laser damage resistance. Opt Express. 2021;29(2):2669–78.
[2] Lian X, Yao WD, Liu WL. KNa2ZrF7: A mixed-metal fluoride exhibits phase matchable second-harmonic-generation effect and high laser induced damage threshold. Inorg Chem. 2021;60(1):19–23.
[3] Ling XL, Liu SH, Liu XF. Enhancement of laser-induced damage threshold of optical coatings by ion-beam etching in vacuum environment. Optik. 2020;200:163429.
[4] Kumar S, Shankar A, Kishore N, Mukherjee C, Kamparath R, Thakur S. Laser-induced damage threshold study on $TiO_2/SiO_2$ multilayer reflective coatings. Indian J Phys. 2020;94:105–15.
[5] Lai QY, Feng GY, Yan J. Damage threshold of substrates for nanoparticles removal using a laser-induced plasma shockwave. Appl Surf Sci. 2021;539:148282.
[6] Zhu CQ, Dyomin V, Yudin N. Laser induced damage threshold of nonlinear GaSe and GaSe:In crystals upon exposure to pulsed radiation at a wavelength of 2.1 μm. Appl Sci-Basel. 2021;11(3):1208.
[7] Xu C, Yi P, Fan HL, Qi JW, Yang S, Qiang YH, et al. Preparation of high laser-induced damage threshold $Ta_2O_5$ films. Appl Surf Sci. 2014;309:194–9.
[8] Chen L, Lu JY, Wu JY, Feng CG. Laser supported detonation wave. Beijing: National Defence Industry Press; 2011.
[9] Nielsen PE, Canavan GH. Electron cascade theory in laser-induced breakdown of preionized gases. J Appl Phys. 1973;44(9):4224–5.
[10] Young M, Hercher M. Dynamics of laser-induced breakdown in gases. J Appl Phys. 1967;38(11):4393–400.
[11] Mori K, Komurasaki K, Katsurayama H. Laser produced plasma in high-speed flows. 24th International Congress on High-speed Photography and Photonics. Vol. 4183. 2001. p. 829–36 (SPIE-4183).
[12] Kim JU, Lee HJ, Kim C. Characteristics of laser-produced plasmas in a gas filled chamber and in a gas jet by using a long pulse laser. J Appl Phys. 2003;94(9):5497–503.
[13] Zhou J, Feng LW, Liu Y, Xu ZH. Laser-induced plasma by high speed photography. J Appl Opt. 2011;32(5):1027–31.
[14] Liu YF, Ding YJ, Peng ZM, Huang Y, Du Y-J. Spectroscopic study on the time evolution behaviors of the laser-induced breakdown air plasma. Acta Phys Sin. 2014;63(20):205205.
[15] Yang ZF, Wei WF, Han JX, Wu J, Li XW, Jia SL. Experimental study of the behavior of two laser produced plasmas in air. Phys Plasmas. 2015;22(7):073511.
[16] Liu JH, Lu JZ, Lei JJ, Gao X, Lin JQ. Effect of ambient gas pressure on characteristics of air plasma induced by nanosecond laser. Acta Phys Sin. 2020;69(5):057401.
[17] Wang GX, Su JH. Study on the impulse mechanism of optical films formed by laser plasma shock waves. Open Phys. 2023;21:20220237.
[18] Wang GX, Su JH. Study of the length and influencing factors of air plasma ignition time. Open Phys. 2022;20:740–9.
[19] Wang GX, Su JH, Xu JQ, Wang QS. Study of the flash ignition time of air plasma formed through laser-induced breakdown. Optoelectron Adv Mat. 2018;12:394–400.